BENIN JOURNAL OF PHYSICAL SCIENCES
BJPS Vol. 1(2), December, pg. 131-144 (2024)
ISSN 3043-6931(Print)
3043-694X(Online)
www.bjps.org.ng

Design of a High Gain Dual-Band Compact Slotted Microstrip Patch Antenna for 5G Mobile Communication Systems

M. A. YUSUF[1] and M. H. ALI[2]
[1]*Department of Physics, Abubakar Tafawa Balewa University, Bauchi, Nigeria*
[2]*Department of Physics, Bayero University, Kano, Nigeria*

Received: 04/11/2024 ***Accepted:*** 23/12/2024

Abstract

Microstrip patch antennas (MPAs) are widely used in wireless communication systems due to their low cost, compact profile, and ease of fabrication. However, their limited gain and narrow bandwidth often restrict their applications. With fifth-generation (5G) networks demanding compact, high-gain, and wide bandwidth antennas, this work presents dual-band Microstrip Rectangular Patch Antennas featuring LI-shaped and middle slots, specifically designed to enhance gain and bandwidth for 5G mobile communication applications. Inserting slots into a unified rectangular patch antenna led to significant gain and bandwidth enhancements, effectively meeting the demands of 5G Systems. The study utilizes the Computer Studio Suite (CST) for simulation, optimizing slot dimensions to achieve the best performance. The newly designed patch antennas were thoroughly evaluated and compared with previous microstrip patch array antenna designs targeting the 26 GHz and 28 GHz frequency bands. The proposed antennas exhibited substantial gain and directivity, wide bandwidth, an optimal Voltage Standing Wave Ratio (VSWR), and high efficiency at the specified resonance frequencies. These designs show promise in advancing the integration of 5G capabilities in hand-held devices, as the antennas' weight and size are significantly reduced.

Keywords: 5G, Antenna bandwidth, Antenna gain, Microstrip antennas, Slot antennas

1. INTRODUCTION

In the period of widespread 5G network deployment, there is a pressing need for antennas that excel in performance, fully leveraging the potential of millimeter-wave frequencies. The frequency bands for 5G communication extend from 24.25 to 27.5 GHz, 27.5 to 29.5 GHz, 37 to 40 GHz, and 64 to 71 GHz. Regional disparities in frequency band selection exist, with China and Europe preferring

*Corresponding author e-mail: yamuhammad@atbu.edu.ng

the 26 GHz range. South Korea, Japan, and the US lean towards the 28 GHz band for their 5G rollouts. The essence of 5G lies in achieving high data rates alongside low-latency communication, and MPAs have emerged as promising candidates to meet these demands. As technological progress advances, these antennas are progressively being integrated into 5G mobile communication equipment, as demonstrated by the research (Nafea and Khamiss, 2023).

Microstrip patch antennas, known for their compatibility with unified circuit technology, low-profile design, compact size, lightweight, and affordability, have become essential in many systems for wireless communication like GPS, RFID, and portable phones. With the continuous progress of technology, especially with the emergence of 5G applications, researchers are progressively focusing on increasing the radiation features of MPAs to satisfy the demands of contemporary communication networks better (Nahas, 2022a). This enhancement is often realized through microstrip patch arrays, which offer superior performance in beam routing, bandwidth, gain, directivity, and flexibility to precise application necessities. Thus, they are widely preferred in many radar and communication systems.

Nevertheless, despite their superior gain and bandwidth characteristics, microstrip patch arrays' intricacy and enlarged size make such designs less practical for numerous applications, especially in hand-held devices like phones. Consequently, various efforts have been undertaken to address these challenges.

In Abdelaziz and Hamad (2019), a tri-band line-fed MPA for multi-band 5G wireless communication applications was introduced. The design offers gains of 5.67 dB at 10 GHz, 9.33 dB at 28 GHz, and 9.57 dB at 38 GHz. In Gemeda et al. (2021), a MPA for 5G communication networks at 28 GHz was presented. The simulated results indicated a return loss of -38.86 dB, bandwidth of 1.046 GHz, gain of 7.587 dB, directivity of 7.509 dBi, and radiation efficiency of 98.214%. Similarly, in Didi et al. (2022) for 5G wireless applications, a rectangular MPA with a rectangular slot operating at 28 GHz was presented, using the microstrip line technology for feeding. The results revealed the antenna resonated at 27.97 GHz, with a reflection coefficient of -20.95 dB, bandwidth of 1.06 GHz, a gain of 7.5 dB, and efficiency of 99.83%. In Rana and Smieee (2022), a MPA operating at 28 GHz was studied and modeled for present 5G communication technologies. The simulation results showed a return loss of -38.348 dB, gain of 8.198 dB, VSWR of 1.02, and efficiency of 77%. In Nahas (2022a), an L-slotted super high gain MPA was developed for 5G portable systems resonating at 26 and 28 GHz, achieving maximum gains of 8.63 and 11.26 dB respectively. Similarly, in Nahas (2022b) an LI-slotted high-gain dual-band MPA was designed for 5G portable communication devices, achieving peak gains of 8.68 dB at 26.28 GHz, and 11.23 dB at 28.54 GHz. Furthermore, in Yusuf and Ali (2024) a slotted single-band high-

gain MPA for 5G applications was reported. The results indicated the highest gain of 9.26 dB and directivity of 10.00 dBi at 28 GHz. With the increasing demand for smaller sizes in hand-held devices, there is a critical need for compactly packed microstrip patch antennas that provide remarkably high gain and wide bandwidth. This is essential for efficiently integrating them into 5G applications instead of using arrays.

This paper aimed to introduce a dual-band MRPA with a patch structure optimized for operation within the mm-wave 5G bands at 26 GHz and 28 GHz. The objective is to substantially improve antenna gain and bandwidth by employing a more advanced slotted patch approach and conducting a comparative analysis with previously developed microstrip patch array antennas.

1.1 Background Theory

The area of a strip of width $rd\theta$ protracted round a sphere at a constant angle θ is given by $(2\pi r \sin\theta)\,(rd\theta)$. Integrating the expression for θ values from 0 to π produces the area of the sphere. Hence,

$$\text{Area of sphere} = 4\pi r^2 \tag{1}$$

where 4π = solid angle protracted by a sphere.

Forthwith, the beam area or beam solid angle Ω_A for an antenna is given by the integral of the stabilized power pattern over a sphere

$$\Omega_A = \int_0^{2\pi}\int_0^{x} P_n(\theta,\emptyset)d\Omega \tag{2}$$

Directivity (D) is calculated from:

$$D = \frac{4\pi}{\Omega_A} \tag{3}$$

where Ω_A = beam solid angle

The lower the beam's solid angle, the higher the directivity.

Gain (G) is given by:

$$G = kD \tag{4}$$

where *k* = efficiency factor of the antenna (Kraus, 1997).

A MPA comprises of a radiating patch positioned on a dielectric substrate, with a ground plane on the opposite side. Electromagnetic waves emanate from the upper portions of the patch into the substrate, reflecting off the ground plane and radiating into the air. Numerous shapes, including circular, elliptical, square, and rectangular, can be used for MPA. In this study, the rectangular shape is chosen for its easiness and widespread use, as depicted in Figure 1.

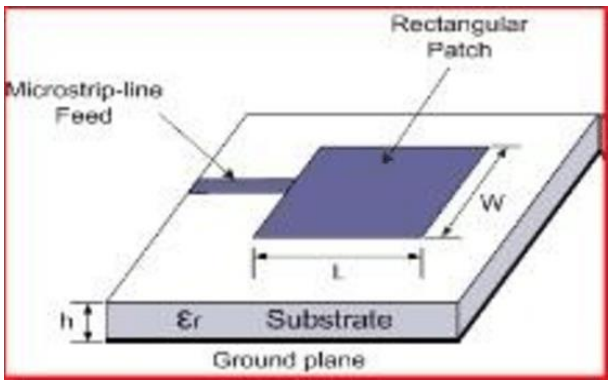

Figure 1: *A Rectangular Microstrip Patch Antenna (Deepika et al., 2017)*

In microstrip patch antenna design, selecting the dielectric substrate, substrate thickness, and resonant frequency is critical. These selections dictate many other parameters, such as patch dimensions and feed location, which can be calculated using equations (5-10) (Nafea and Khamiss 2023).

The width of the patch (W_p) can be written as:

$$W_p = \frac{c}{2f_o}\sqrt{\frac{2}{\varepsilon_r+1}} \tag{5}$$

where c is the velocity of free space, f_o is resonate frequency, and ε_r is the dielectric constant of the substrate.

and the effective dielectric constant (ε_{reff}) is given by:

$$\varepsilon_{reff} = \frac{\varepsilon_r+1}{2} + \frac{\varepsilon_r-1}{2}\left[1+12\frac{h}{W_p}\right]^{-1/2} \tag{6}$$

where h is the height of the dielectric substrate

while the extension in length (ΔL) is given by:

$$\Delta L = 0.412h\left[\frac{(\varepsilon_{reff}+0.3)\left(\frac{W_p}{h}+0.264\right)}{(\varepsilon_{reff}-0.258)\left(\frac{W_p}{h}+0.8\right)}\right] \tag{7}$$

The length of the patch (L_p) is given by:

$$L_p = L_{eff} - \Delta L \tag{8}$$

$$\text{where } L_{eff} = \frac{c}{2f_0\sqrt{\varepsilon_{reff}}}$$

while the length of the substrate (L_s) is given by:

$$L_s = 6h + L_p \tag{9}$$

and finally, the width of the substrate (W_s) is given by:

$$W_s = 6h + W_p \tag{10}$$

2. MATERIALS AND METHOD

2.1 Material

The material used in this research is CST Studio Suite Version 2018 software.

2.2 Method (Antenna Design)

This study adopts a design approach that focuses on rectangular patch antennas, similar to Nahas and Nahas (2019); Nahas (2022b); Yusuf and Ali (2024). The chosen antennas feature a rectangular patch with slots of LI, combinations, and some appropriate mid-shapes to enhance better ascendance over the gain and other radiation performance. These antennas are constructed on Rogers RT5880 substrate, with specified dimensions of 16.5 mm length, 20 mm width, and 0.508 mm thickness, along with a loss tangent (tan δ) of 0.0009 and a relative dielectric permittivity (ε_r) of 2.2. For additional details regarding the Rogers RT/Duroïd 5880 substrate characteristics, refer to (Abdelaziz and Hamad 2019). Here, inset feeding is utilized as the preferred technique among various feeding methods in MPAs, aiming for optimal impedance matching between the patch and the feeding line. The patch is 9.7 × 9.9 mm² in size and is fed via a microstrip line that is 4.75 mm long and 0.7 mm wide 50 Ω. Table 1 presents the optimum values of the inset-fed and different slots for the dual-band antennas as depicted in Figures 2(a-c).

Table 1: *Optimum values of the slots and inset-feds of the antenna design (in millimeters).*

Parameter	SL_I	SW_I	SL_2	SW_2	SL_3	SW_3	SL_4	SW_4	SL_5	SW_5	Y_O	X_O
(a)	0.75	1.75	5.05	0.75	4.90	0.85	1.00	3.70	2.45	1.20	2.12	0.58
(b)	0.75	1.75	5.05	0.75	4.95	0.85	0.70	4.35	3.00	3.65	2.40	0.60
(c)	0.75	1.75	5.20	0.75	5.05	0.85	4.00	4.20	-	-	2.32	0.60

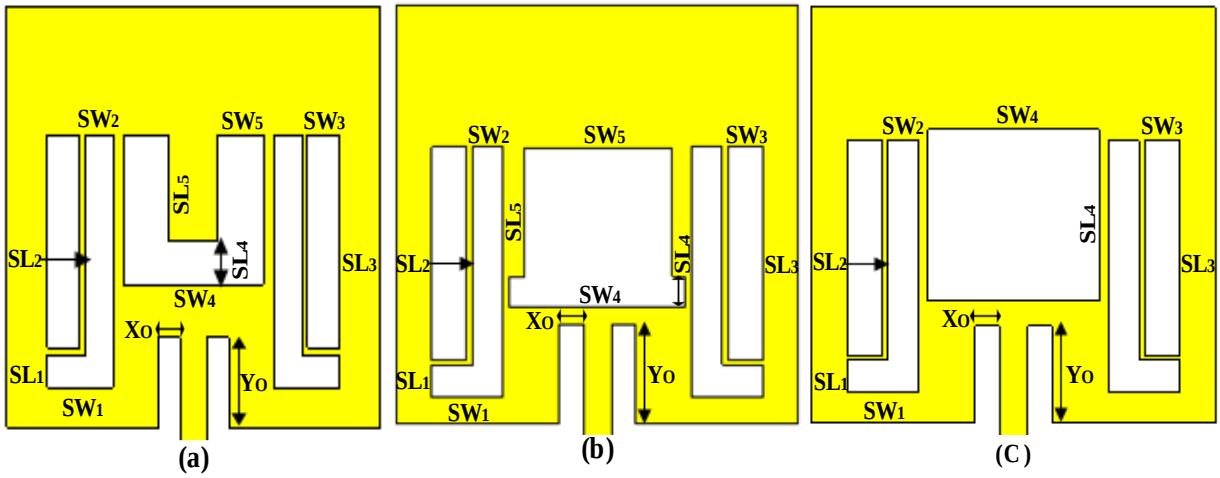

Figure 2: *The design geometry of the inset-fed and slotted patch elements.*

3. RESULT AND DISCUSSION

This part details the simulation outcomes of three (3) advanced slotted patch antenna designs intended to realize the higher gain, and wide bandwidth in the dual 5G bands (26 and 28 GHz), simulated using CST software. Tables 2-4 present the complete findings of the radiation variables selected for this investigation, assessing the effectiveness of the constructed MRPA. These variables comprise a center frequency, reflection coefficient (S_{11}), VSWR, bandwidth, gain, directivity, and efficiency. The results in Table 2 display that the proposed design 2(a) only resonated at 28 GHz.

3.1 Design featuring double LI and middle U slots

Table 2 gives the performance outcomes extracted from Figure 2(a). The antenna performs well, considering its low S_{11} value, wide bandwidth, and high gain in the 28 GHz band. Though, as indicated in Figure 3(a), it does not resonate at the 26 GHz band.

Table 2: *Simulated results of the design depicted in Figure 2(a)*

Resonance Frequency (GHz)	Return loss S_{11} (dB)	Bandwidth (GHz)	VSWR	Gain (dB)	Directivity (dBi)	Efficiency (%)
28.00	-44.95	1.09	1.01	10.13	11.07	92.00

Yet, improvements may be required for the gain, directivity, and efficiency to align with the emerging design requirements for 5G. This can be attained by integrating various centrally positioned slot elements into the dual LI-shaped slots selected in the innovative design. Figure 3(a) displays the S_{11} and bandwidth, Figure 3(b) illustrates the VSWR, while Figures 4(a) and 4(b) demonstrate the gain and directivity at 28 GHz.

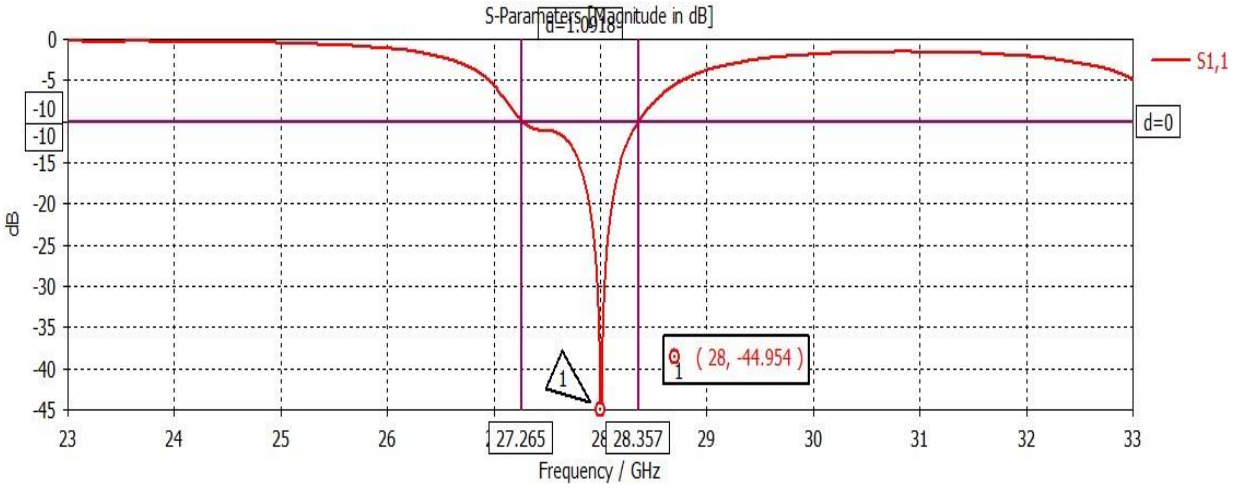

Figure 3(a): *Return loss (S_{11}) and Bandwidth as functions of frequency for design 2(a).*

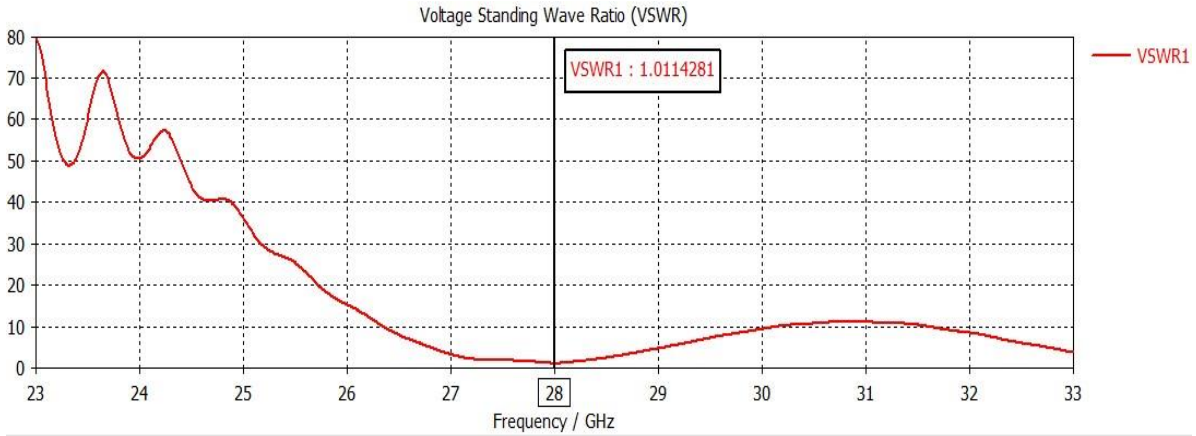

Figure 3(b): *VSWR parameter as a function of frequency for design 2(a)*

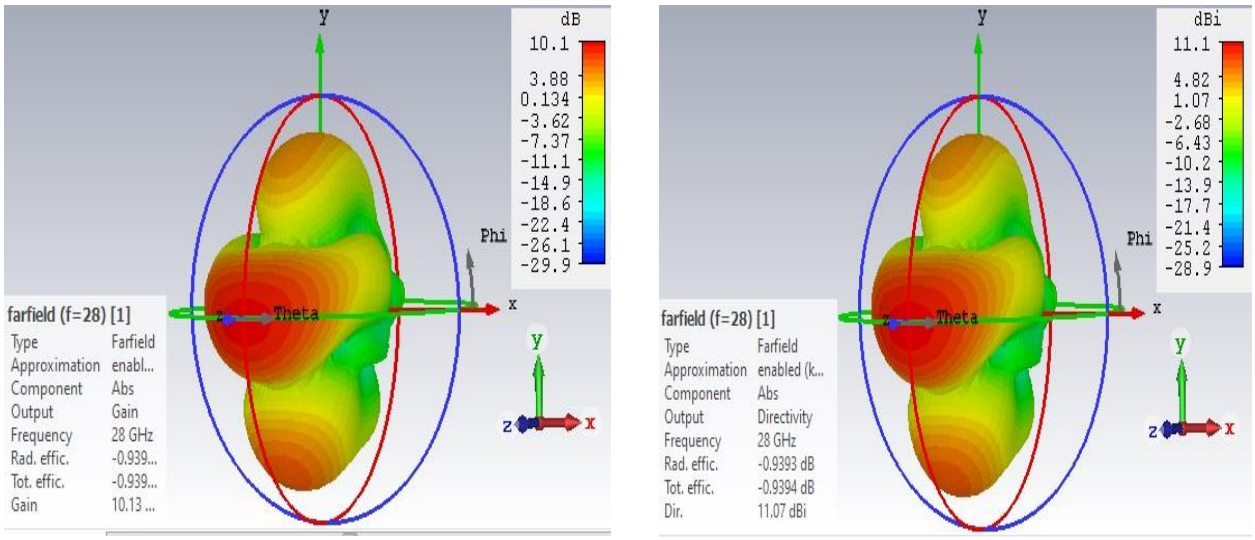

(a) (b)

Figure 4: *Gain and directivity for the proposed antenna design 2(a)*

3.2 Design featuring dual LI and centrally positioned 𝐼 slots.

The results from Figure 2(b), summarized in Table 3, demonstrate improvements in gain, directivity, and efficiency at 28 GHz. Specifically, design 2(b) achieves resonance at 26 GHz with excellent VSWR, gain, directivity, and efficiency values. Though the bandwidth is not extremely broad in both cases, it is still deemed adequate for 5G applications. Despite having the lowest bandwidth, the reflection coefficient value is outstanding, as shown in Figure 5(a), remaining well below the -10 dB limit across all designs. The VSWR, depicted in Figure 5(b), indicates good impedance matching between the antenna and its feeding system. Figures (6a) and (6b) demonstrate the gain and directivity at 26 GHz, while Figures 7(a) and 7(b) demonstrate the gain and directivity at 28 GHz, respectively.

Table 3: *Simulated results of the design depicted in Figure 2(b)*

Resonance Frequency (GHz)	Return loss S_{11} (dB)	Bandwidth (GHz)	VSWR	Gain (dB)	Directivity (dBi)	Efficiency (%)
26.24	-16.10	0.44	1.37	8.13	8.49	96.00
28.00	-36.46	0.97	1.03	11.16	11.88	94.00

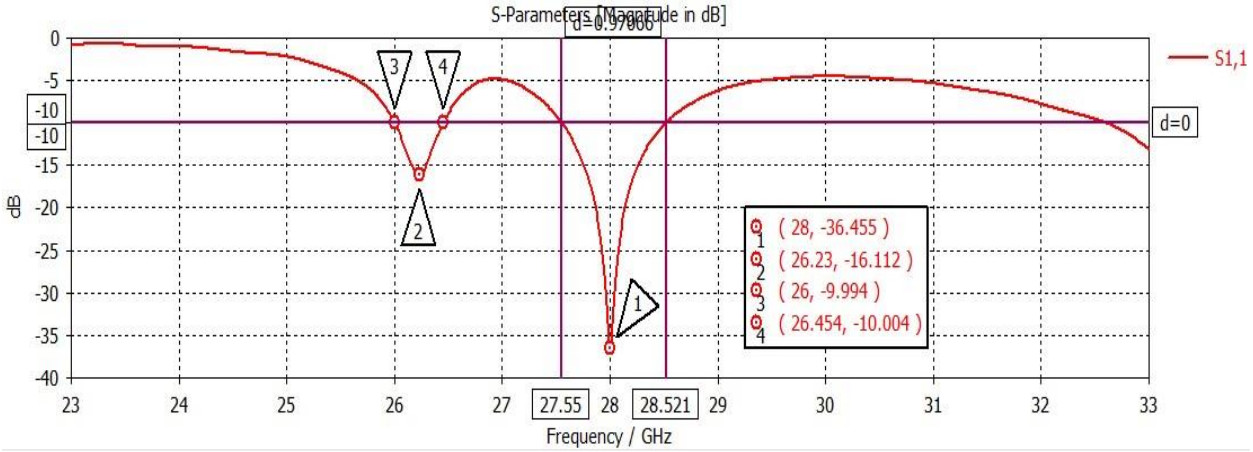

Figure 5(a): *Return loss (S_{11}) and Bandwidth as functions of frequency for design 2(b)*

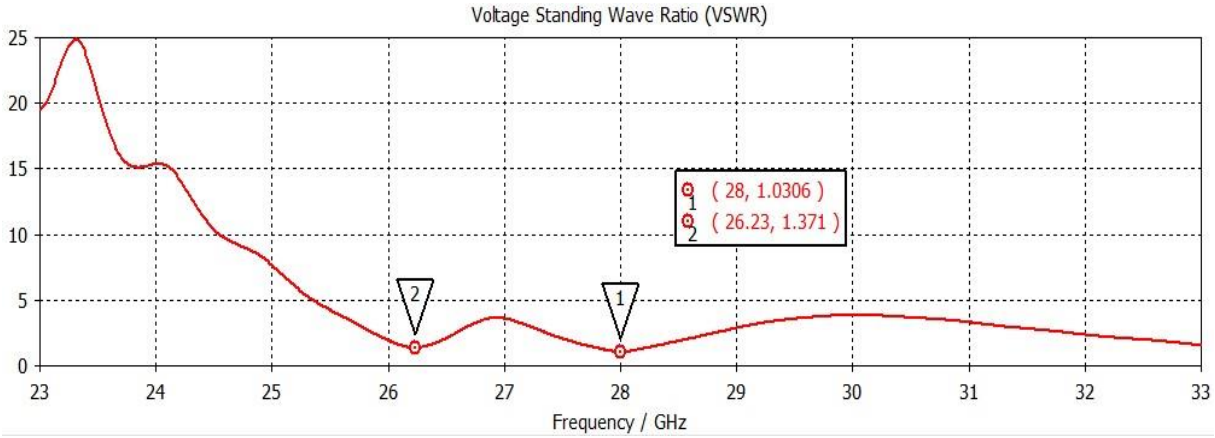

Figure 5(b): *VSWR parameter as a function of frequency for design 2(b)*

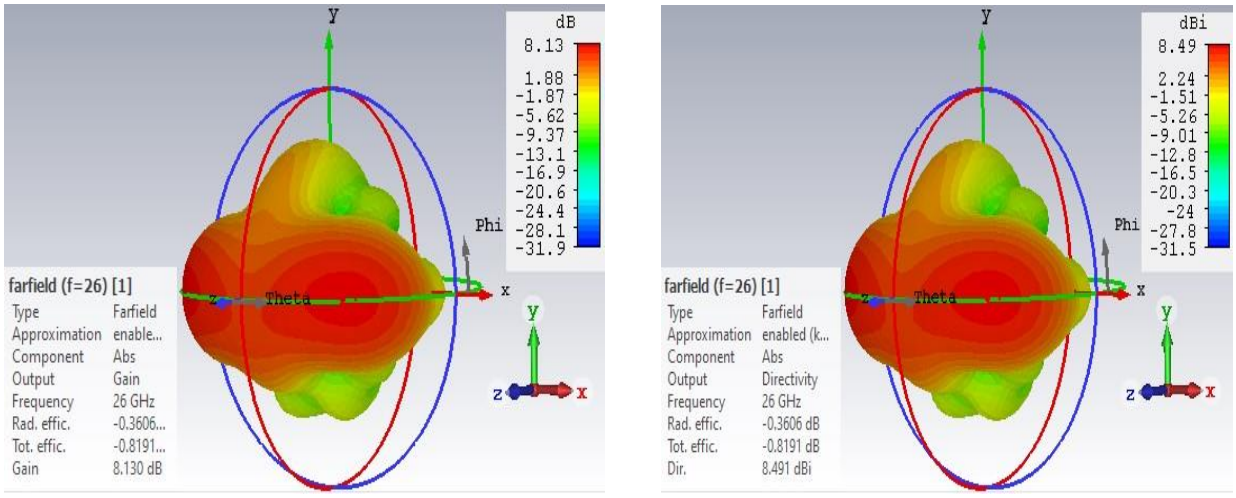

(a) (b)

Figure 6: *Gain and directivity for the proposed antenna design 2(b) at 26 GHz*

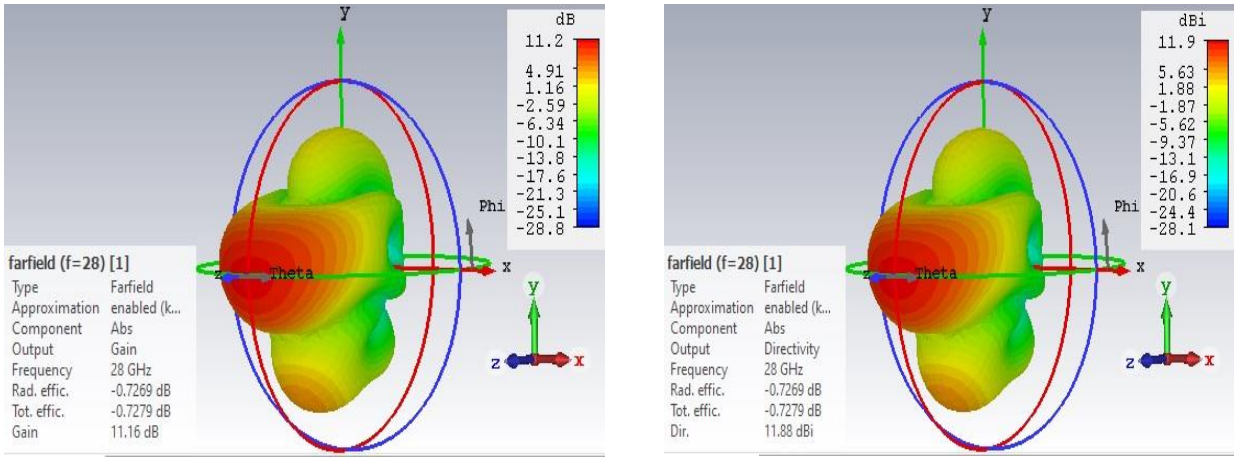

(a) (b)

Figure 7*: Gain and directivity for the proposed antenna design 2(b) at 28 GHz*

3.3 Design featuring double LI-shape and centrally positioned rectangular slots

In MPA design, simplicity is vital but can occasionally compromise radiation performance. To improve this, design 2(c) employed a rectangular slot positioned in the center to enhance radiation performance, especially gain and directivity. The results in Table 4 indicate that this design improved the antenna's radiation performance, boosting directivity and gain at both 5G bands. Additionally, there was no compromise in efficiency at 28 GHz despite the enhancement in gain and directivity.

When comparing the previous two designs, the bandwidth of the antenna design at 28 GHz, which is 1.08 GHz, is greater than that gained from design 2(b) and is deemed suitable for 5G applications. Figure 8(a) displays the S_{11} and bandwidth parameters, while Figure 8(b) shows the VSWR.

Figures 9(a) and 9(b) illustrate the gain and directivity at 26 GHz, while Figures 10(a) and 10(b) show the gain and directivity at 28 GHz, respectively.

Table 4: *Simulated results of the design depicted in Figure 2(c)*

Resonance Frequency (GHz)	Return loss S_{11} (dB)	Bandwidth (GHz)	VSWR	Gain (dB)	Directivity (dBi)	Efficiency (%)
26.75	-22.63	0.54	1.16	8.99	9.64	93.00
28.00	-23.58	1.08	1.14	11.37	12.10	94.00

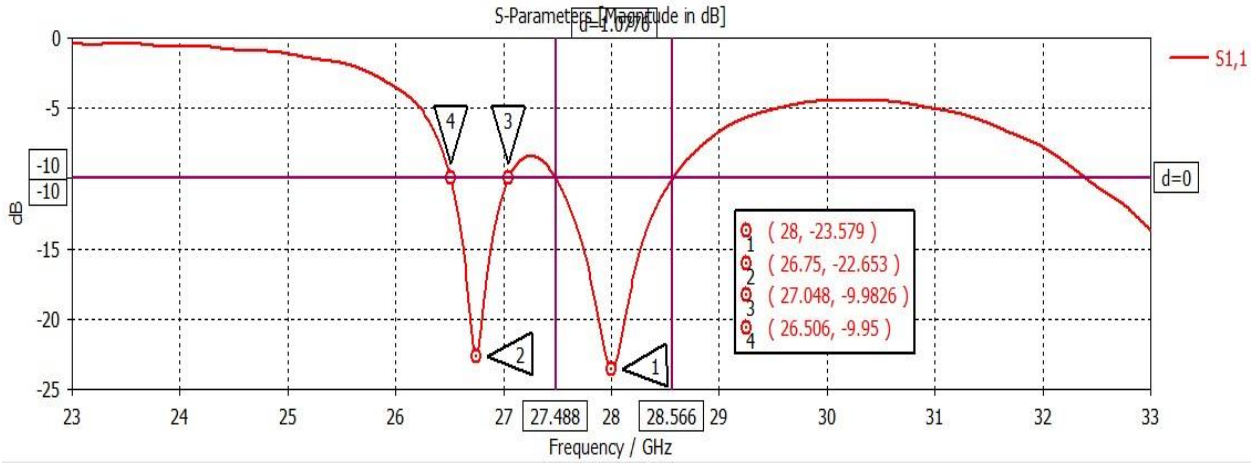

Figure 8(a): *Return loss (S_{11}) and Bandwidth as functions of frequency for design 2(c)*

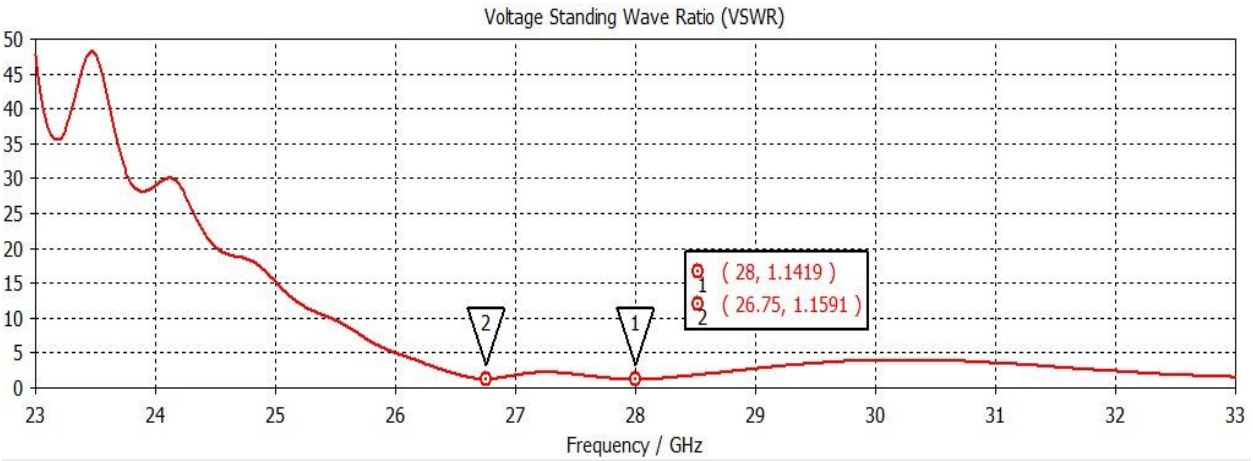

Figure 8(b): *VSWR parameter as a function of frequency for design 2(c)*

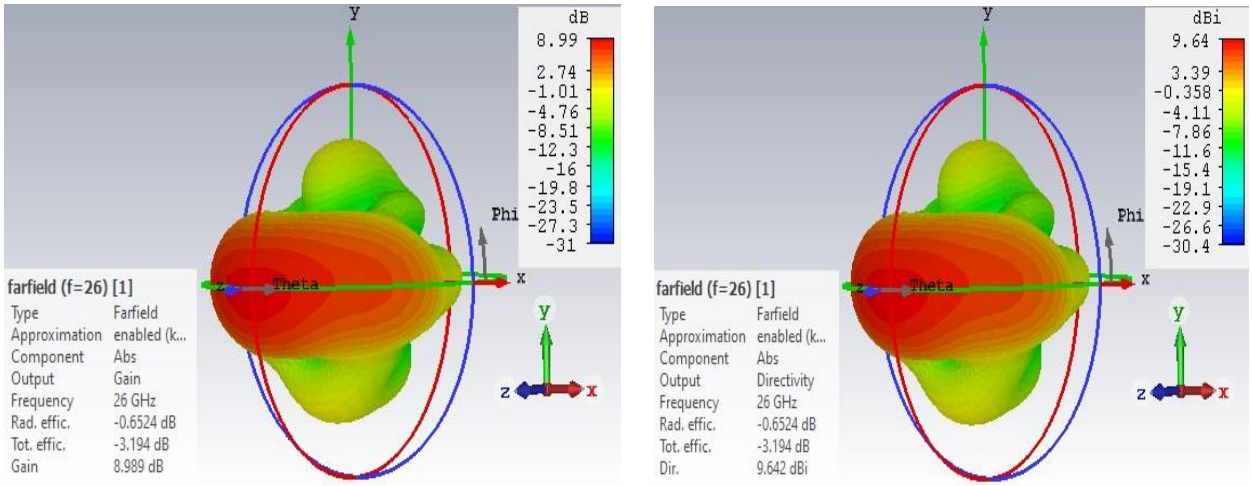

(a) (b)

Figure 9: *Gain and directivity for the proposed antenna design 2(c) at 26 GHz*

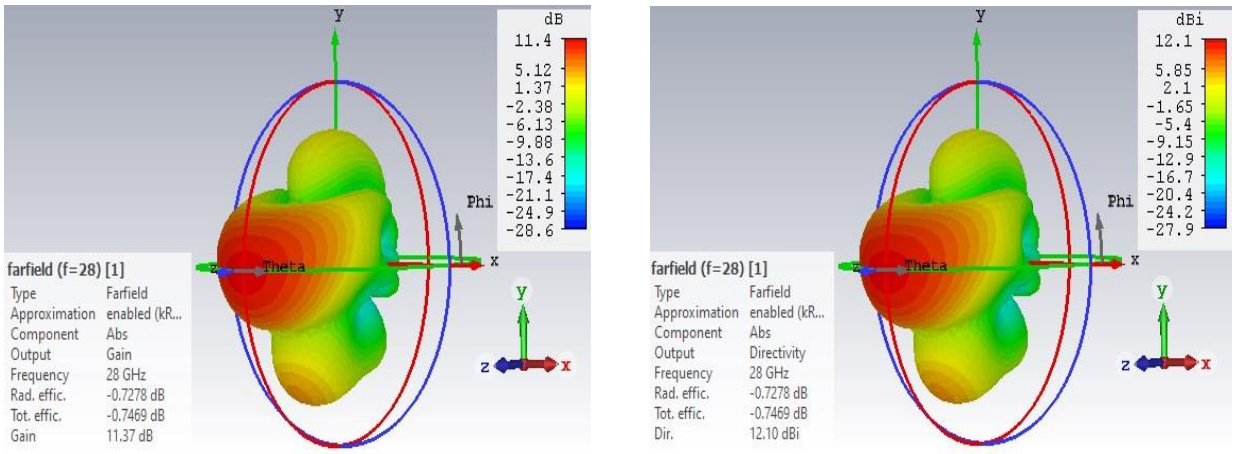

(a) (b)

Figure 10: *Gain and directivity for the proposed antenna design 2(c) at 28 GHz*

3.4 Evaluation of the simulated designs with previous array antenna designs

Table 5 presents a relative study of the performance of the three simulated antennas with a collection of earlier published array designs from the literature. These designs utilized array patch configurations with a resonant frequency of ≥ 28 GHz, targeting high gain for 5G applications. The results are arranged in descending order, highlighting the gain values for easy reference.

Table 5: *Comparison of proposed designs with different arrays at the 28 GHz band.*

References	No. of Antennas	Frequency (GHz)	Minimum S_{11} (dB)	BW (GHz)	VSWR	Gain (dB)	Directivity (dBi)	Efficiency (%)
This work (2c)	Single	28.00	-23.58	1.14	1.08	11.37	12.10	94.00
(Bakry et. al., 2018)	4×1	28.00	-21.44	-	1.65	11.23	11.99	94.00
This work (2b)	Single	28.00	-36.46	0.97	1.03	11.16	11.88	94.00
This work (2a)	Single	28.00	-44.95	1.09	1.01	10.13	11.07	92.00
(Didi et al., 2021)	2×2	27.078	-31.70	1.05	1.07	10.60	11.20	95.00
(Didi et al., 2023)	1×2	28.00	-35.91	1.03	1.43	9.42	9.50	99.80
(Hakim et al., 2020)	2×2	28.00	-54.00	5.13	1.00	8.31	8.35	98.00
(Marzouk, 2020)	1×2	27.946	-27.84	2.30	1.08	7.18	7.58	91.24

Based on the analysis of the results presented in Table 5, it is apparent that our simulated antenna in design 2(c) surpasses all earlier studied antennas, showing higher gain and directivity. Precisely, the peak gain and directivity reached remarkable values of 11.37 dB and 12.10 dBi, respectively. Impressively, other important parameters remain uncompromised compared to different designs, excluding bandwidth and efficiency, which were slightly forfeited to achieve excellent gain and directivity. Designs 2(a) and 2(b) also excel over many others in the literature except the one published in (Bakry et al. 2018). Other metrics, like efficiency, VSWR, and return loss, demonstrate robust performance compared to other designs.

4. CONCLUSION

This study used various slots to design a high-gain, dual-band compact MPA suitable for 5G mobile communication services. The primary concept was to increase antenna gain, directivity, and bandwidth using CST software. Three (3) slotted microstrip antenna designs were proposed, concentrating on a single-patch configuration for operation at 26 and 28 GHz. The proposed designs, particularly

the LI and central rectangular-slotted design, showed higher gain and directivity than existing array designs, with peak values of 11.37 dB and 12.10 dBi, respectively. These values surpassed the 11.23 dB gain and 11.99 dBi directivity achieved by (Bakry et al. 2018). Other radiation parameters like VSWR, reflection coefficient, and efficiency also exhibited commendable performance. These findings reveal that the proposed slotted MPA designs are compact, simple, and cost-effective, suitable for smooth integration into handheld devices for 5G applications.

CONFLICT OF INTEREST

No conflict of interest was declared by the author.

REFERENCES

[1] Abdelaziz, A., Ehab, K. I., and Hamad. (2019). Design of a Compact High Gain Microstrip Patch Antenna for Tri-Band 5G Wireless Communication. *Frequenz,* 73(1–2), 45–52. doi: 10.1515/freq-2018-0058.

[2] Bakry, M., Mashade, E. L. and Hegazy, E. A. (2018). Design and Analysis of 28GHz Rectangular Microstrip Patch Array Antenna. *WSEAS TRANSACTIONS on COMMUNICATIONS,* 17, 1–9. doi: E-ISSN: 2224-2864.

[3] Deepika, J., Mathivanan, M., Muruganandham, A. and Vivek, R. (2017). Parametrical Variation and Its Effects on Characteristics of Microstrip Rectangular Patch Antenna. *Proceedings of the 2nd IEEE International Conference on Electrical, Computer and Communication Technologies, ICECCT* (November). doi: 10.1109/ICECCT.2017.8117913.

[4] Didi, S., Imane, H., Abdelhafid, E., Mohammed, F., Younes, B., and Moulhime, E. (2023). New Microstrip Patch Antenna Array Design at 28 GHz Millimeter-Wave for Fifth-Generation Application. *International Journal of Electrical and Computer Engineering (IJECE),* 13(4), 4184–4193. doi: 10.11591/ijece.v13i4.pp4184-4193.

[5] Didi, S., Imane, H., Mohammed, F., Younes, B., Moulhime, E., and Salah-eddine, D. (2022). Design of a Microstrip Antenna Patch with a Rectangular Slot for 5G Applications Operating at 28 GHz. *TELKOMNIKA Telecommunication Computing Electronics and Control,* 20(3), 527–536. doi: 10.12928/TELKOMNIKA.v20i3.23159.

[6] Gemeda, M. T., Kinde, A. F., Hana, L. G., and Ayane, L. G. (2021). Design and Analysis of a 28 GHz Microstrip Patch Antenna for 5G Communication Systems. *International Research Journal of Engineering and Technology (IRJET)* 08(02), 881–886.

[7] Hakim, M. L., Mohammed, J. U., and Md, J. H. (2020). 28/38 GHz Dual-Band Microstrip Patch Antenna with DGS and Stub-Slot Configurations and Its 2*2 MIMO Antenna Design for 5G Wireless Communication. *2020 IEEE Region 10 Symposium, TENSYMP 2020* (June), 56–59. doi: 10.1109/TENSYMP50017.2020.9230601.

[8] Kraus, J. D. and Marhefka J. R. (1997). *Antennas-for-All-Applications*. Sixth. Tata McGraw-Hill Publishing Companies, inc. New York.

[9] Marzouk, S. and Ahmed, M. (2020). A Two-Element Microstrip Antenna 28/38 GHz For 5G Mobile Applications. *Delta University Scientific Journal*, 3(1), 1–8. doi: 10.35360/njes.34.

[10] Nafea, S. N. and Nasser, N. K. (2023). For 5G Applications, High-Gain Patch Antenna in Ka-Band. *Indonesian Journal of Electrical Engineering and Computer Science*, 31(2), 802–809. doi: 10.11591/ijeecs.v31.i2.pp802-809.

[11] Nahas, M. (2022a). A Super High Gain L-Slotted Microstrip Patch Antenna For 5G Mobile Systems Operating at 26 And. *Engineering, Technology & Applied Science Research*, 12(1), 8053–8057.

[12] Nahas, M. (2022b). Design of a High-Gain Dual-Band LI-Slotted Microstrip Patch Antenna for 5G Mobile Communication Systems. *Journal of Radiation Research and Applied Sciences*, 15(4), 100483. doi: 10.1016/j.jrras.2022.100483.

[13] Nahas, M. M. and Mouaaz, N. (2019). Bandwidth and Efficiency Enhancement of Rectangular Patch Antenna for SHF Applications. *Engineering, Technology and Applied Science Research*, 9(6), 4962–4967. doi: 10.48084/etasr.3014.

[14] Rana, Sohel, and Mostafizur Rahman Smieee. (2022). Design and Analysis of Microstrip Patch Antenna for 5G Wireless Communication Systems. *Cogent Engineering*, 11(6), 1–15. doi: 10.11591/eei.v11i6.3955.

[15] Didi, S., Halkhams, I., Fattah, M., Balboul, Y., Mazer, S., El Bekkali, M. and Rabia Ç. (2021). Study and Design of Printed Rectangular Microstrip Antenna Arrays at an Operating Frequency of 27.5 GHz for 5G Applications. *Journal of Nano and Electronic Physics*, 13(6), 1–5. doi: 10.21272/jnep.13(6).06035.

[16] Yusuf, M. A., and Ali., M. H. (2024). Simulation of High-Gain Microstrip Patch Antennas for 5G Applications. *Dutse Journal of Pure and Applied Sciences (DUJOPAS)*, 10(1), 130–39.